scientific reports

Check for updates

OPEN

Desiccation-induced fibrous condensation of CAHS protein from an anhydrobiotic tardigrade

Maho Yagi-Utsumi[1,2,3], Kazuhiro Aoki[1,4], Hiroki Watanabe[1], Chihong Song[1,5], Seiji Nishimura[3], Tadashi Satoh[3], Saeko Yanaka[1,2,3], Christian Ganser[1], Sae Tanaka[1,6], Vincent Schnapka[2,7,12], Ean Wai Goh[2], Yuji Furutani[2,13], Kazuyoshi Murata[1,5], Takayuki Uchihashi[1,8,9], Kazuharu Arakawa[1,6,10,11] & Koichi Kato[1,2,3]✉

Anhydrobiosis, one of the most extensively studied forms of cryptobiosis, is induced in certain organisms as a response to desiccation. Anhydrobiotic species has been hypothesized to produce substances that can protect their biological components and/or cell membranes without water. In extremotolerant tardigrades, highly hydrophilic and heat-soluble protein families, cytosolic abundant heat-soluble (CAHS) proteins, have been identified, which are postulated to be integral parts of the tardigrades' response to desiccation. In this study, to elucidate these protein functions, we performed in vitro and in vivo characterizations of the reversible self-assembling property of CAHS1 protein, a major isoform of CAHS proteins from *Ramazzottius varieornatus*, using a series of spectroscopic and microscopic techniques. We found that CAHS1 proteins homo-oligomerized via the C-terminal α-helical region and formed a hydrogel as their concentration increased. We also demonstrated that the overexpressed CAHS1 proteins formed condensates under desiccation-mimicking conditions. These data strongly suggested that, upon drying, the CAHS1 proteins form oligomers and eventually underwent sol–gel transition in tardigrade cytosols. Thus, it is proposed that the CAHS1 proteins form the cytosolic fibrous condensates, which presumably have variable mechanisms for the desiccation tolerance of tardigrades. These findings provide insights into molecular strategies of organisms to adapt to extreme environments.

Anhydrobiosis is one of the most extensively studied forms of cryptobiosis that is induced in response to desiccation conditions in certain organisms, including bacteria, fungi, plants, and animals[1–4]. Even after almost complete dehydration, anhydrobiotic organisms do not exhibit irreversible protein denaturation and aggregation. The organisms in anhydrobiotic states can tolerate desiccation for decades while maintaining their resuscitation ability[5]. In this state, they are also cross-tolerant to various environmental stresses caused by extremely high and low temperatures, high and low pressures, and radiation[6–8]. Therefore, a deeper understanding of the mechanisms behind the anhydrobiosis has versatile applications to develop technologies to endow molecular systems, cells, and tissues of clinical and industrial interest with resistance against various environmental stresses.

It has been hypothesized that anhydrobiotic species accumulate substances which can protect their biological components or cell membrane without water. Early studies on desiccation tolerance identified the disaccharide trehalose and the late embryogenesis abundant (LEA) proteins as the functional mediators of anhydrobiosis[9].

[1]Exploratory Research Center on Life and Living Systems (ExCELLS), National Institutes of Natural Sciences, 5-1 Higashiyama, Myodaiji, Okazaki, Aichi 444-8787, Japan. [2]Institute for Molecular Science (IMS), National Institutes of Natural Sciences, Okazaki, Aichi 444-8787, Japan. [3]Graduate School of Pharmaceutical Sciences, Nagoya City University, Nagoya, Aichi 465-8603, Japan. [4]National Institute for Basic Biology (NIBB), National Institutes of Natural Sciences, Okazaki, Aichi 444-8787, Japan. [5]National Institute for Physiological Sciences (NIPS), National Institutes of Natural Sciences, Okazaki, Aichi 444-8585, Japan. [6]Institute for Advanced Biosciences, Keio University, Tsuruoka 997-0017, Japan. [7]Ecole Nationale Supérieure de Chimie de Paris, 75005 Paris, France. [8]Department of Physics, Nagoya University, Nagoya 464-8602, Japan. [9]Institute for Glyco-Core Research (iGCORE), Nagoya University, Nagoya 464-8601, Japan. [10]Faculty of Environment and Information Studies, Keio University, Fujisawa 252-0882, Japan. [11]Systems Biology Program, Graduate School of Media and Governance, Keio University, Fujisawa 252-0882, Japan. [12]Present address: Institut de Biologie Structurale, 38044 Grenoble, France. [13]Present address: Department of Life Science and Applied Chemistry, Nagoya Institute of Technology, Nagoya 466-8555, Japan. ✉email: kkato@excells.orion.ac.jp

Trehalose is known to accumulate at high levels under desiccating conditions in many anhydrobiotic organisms, including the larvae of sleeping chironomids *Polypedilum vanderplanki*, cysts of the brine shrimp *Artemia*, and vegetative tissues of the desert resurrection plant *Selaginella*[10–14]. Trehalose is assumed to exert its protective functions through water replacement and vitrification; these are two distinct but not mutually exclusive mechanisms in protecting the organisms from the harmful effects of desiccation[12,15]. In the former mechanism, accumulating trehalose molecules extensively interact with biomolecular surfaces through hydrogen bonds by replacing the water molecules. In the latter mechanism, an amorphous state of trehalose without water vitrifies at a high concentration, preventing the movement of biomolecules, and thereby physically suppresses their denaturation. LEA proteins are a group of intrinsically disordered proteins originally discovered in plant seeds. They have been recently linked to anhydrobiosis in animals, such as nematodes, bdelloid rotifers, and crustaceans[3,9,16,17]. LEA proteins commonly share highly hydrophilic and heat-soluble properties and are supposed to alter their structures from a disordered state to an α-helical state under anhydrous conditions. Hence, LEA proteins have been related to desiccation tolerance with several hypothetical functions, including the stabilization of trehalose vitrification and molecular shielding to prevent protein denaturation and aggregation, regulation of the drying rate as a hydration buffer, and scavenging of divalent metal ions or reactive oxygen species[3,9,18]. Moreover, heat shock proteins like Hsp70 in *Artemia* and *Caenorhadbditis elegans* are speculated to be associated with desiccation-induced misfolding of proteins to prevent their further denaturation and aggregation[1,19,20].

Tardigrades have been studied as typical anhydrobiotic animals, which can exhibit extremotolerance against high and low temperatures, high pressure, and radiation under desiccation conditions[1,21–23]. There have been several reports about the protective mechanisms underlying tardigrade anhydrobiosis, including inductions of heat shock proteins[24], cold shock domain-containing proteins[25], defensive peroxidases[26,27], and stabilization and reorganization of body structure by muscle protein filaments[22,28]. Trehalose accumulation during dehydration was reported for several eutardigrade species, whereas no change in trehalose level was detected in *Milnesiidae* and in heterotardigrades[25,29]. Genomics analyses indicated that not all tardigrade species possess the gene of trehalose-6-phosphatase synthase, a key enzyme in the trehalose biosynthetic pathway[25,30]. These data suggest that the anhydrobiotic ability of tardigrades cannot be explained simply by trehalose accumulation. By contrast, LEA proteins are widely observed in the tardigrade transcriptomes but are not among the most abundant group of transcripts, suggesting the existence of tardigrade-unique components[25,31]. Through heat-soluble proteomics in a search for LEA and LEA-like proteins, highly hydrophilic and heat-soluble protein families have been identified as cytosolic abundant heat-soluble (CAHS) proteins[23,32–34]. Although these proteins are distinct from LEA proteins based on their conserved sequences, they share some similarities with LEA proteins in terms of the bioinformatic prediction of high propensity for α-helix formation[32,33].

The CAHS genes were conserved across all eutardigrada classes such as *Hypsibiidae*, *Macrobiotiidae*, and *Milnesiidae*[25,30,32] while missing in the heterotardigrade lineage[25]. CAHS proteins are constitutively and abundantly expressed in the strong anhydrobiote *Ramazzottius varieornatus*. In contrast, they are strongly induced under desiccation stress in another semiaquatic tardigrade species *Hypsibius exemplaris*; this induction requires de novo gene expression and is indispensable for survival[30,35]. This was subsequently confirmed by RNAi experiments and by the improved desiccation tolerance of yeast and bacterial cells with the heterologous expression of CAHS proteins[34]. While no CAHS homologue has been identified in heterotardigrades, they possess highly abundant heat-soluble proteins that share analogous structural features with CAHS proteins[36]. Hence, despite their limited conservation, the CAHS proteins are expected to provide novel insights into the anhydrobiotic mechanisms.

In view of the situation, we herein conducted in vitro and in vivo characterizations of molecular assembly of CAHS1, a major isoform of CAHS proteins from *R. varieornatus*, using a series of spectroscopic and microscopic techniques.

Results

Fibril formation of the CAHS1 protein in vitro. We first examined molecular structural states of the CAHS1 protein under dehydrating conditions in vitro. The dried CAHS1 proteins on a carbon grid were visualized by transmission electron microscopy (TEM), showing that fibril structures were formed (Fig. 1A). The infrared (IR) spectroscopic analysis showed that the dehydrated CAHS1 protein adopted an α-helical structure (amide I peaks at 1655 cm^{-1} and 1650 cm^{-1}), which was reversibly disrupted upon hydration (Fig. 1B,C). This is consistent with the previous circular dichroism (CD) data, which indicated that the CAHS1 protein adopted helical structures under water-deficient conditions mimicked with trifluoroethanol[32]. These data suggest that the CAHS1 proteins underwent fibrilization coupled with the formation of α-helical structures under desiccating conditions.

Extremotolerant tardigrades undergo body shrink upon drying and eventually become one-fifth the size in anhydrobiotic states, suggesting several-fold increase in protein concentrations during this process. Hence, for a more detailed understanding of this molecular transition, we characterized the assembly of the CAHS1 protein at different concentrations in aqueous solutions. The turbidity of CAHS1 protein solutions increased as the CAHS1 protein concentration increased. Thus, the CAHS1 protein was apt to condensate at higher concentrations (Fig. 1D). In a neutral pH range, the turbidity rose abruptly when the CAH1 protein concentration exceeded 0.3 mM. The CAHS1 protein eventually gelled at a higher concentration (> 0.6 mM) (Fig. 1E) and reversibly turned into a solution upon dilution. These findings indicated that the CAHS1 protein underwent a sol–gel transition in a reversible manner (Fig. 1D,E).

To determine the structural information of its concentration-dependent conformational changes, we performed nuclear magnetic resonance (NMR) spectroscopic analyses of the CAHS1 protein solution. The ^{1}H-^{15}N HSQC spectral data obtained under protein-dilute conditions were similar to those previously reported for CAHS proteins from *H. exemplaris*[34], whose structures were interpreted to be intrinsically disordered (Fig. 2A).

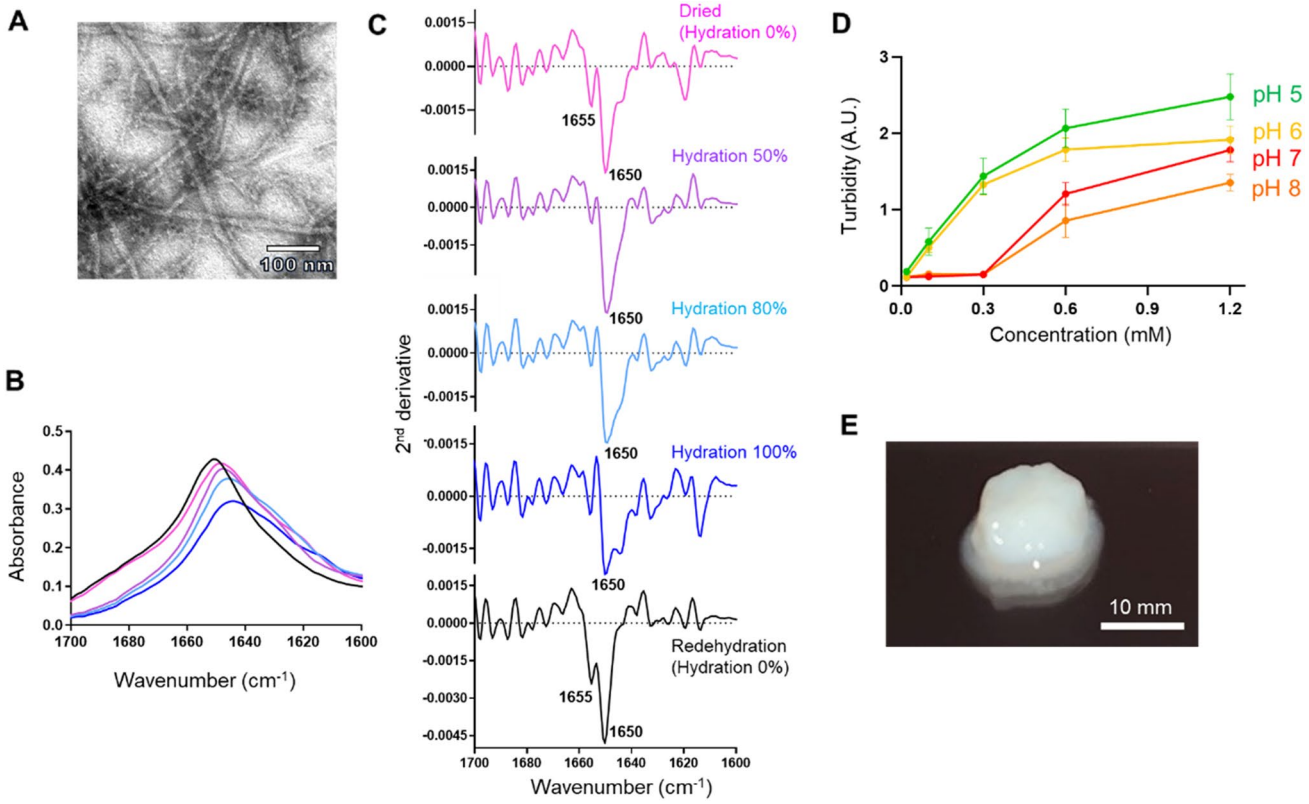

Figure 1. In vitro characterization of the fibrous condensation of CAHS1 proteins. (**A**) TEM image of CAHS1 protein fibrils under dry conditions. (**B**) Amide I band of the CAHS1 protein and (**C**) its second derivative under 0 (magenta), 50 (purple), 80 (cyan), and 100% hydration (D_2O) and dehydration conditions. After 100% hydration (blue), the sample was measured again under redehydration condition (black). (**D**) Turbidity (absorbance at 595 nm) of the CAHS1 protein at 25 °C and pH 5 (green), pH 6 (yellow), pH 7 (red), and pH 8 (orange). The error bars show the standard deviation of three replicates. (**E**) The CAHS1 protein hydrogel formed in 20 mM potassium phosphate buffer (pH 6.0) at 25 °C. The initial protein concentration was 1.2 mM.

We noticed that the HSQC peaks from the CASH1 protein at lower concentrations could be classified into two: extremely narrow and broad ones. We divided the CAHS1 protein from *R. varieornatus* into the N-terminal and C-terminal halves (termed CAHS1-N and CAHS1-C, respectively) and measured their NMR and CD spectra (Supporting Fig. S1A–C). The results indicate that the CAHS1-N and CAHS1-C fragments adopted an intrinsically disordered and α-helical structures, respectively. Furthermore, the NMR spectrum of the CAHS1 protein exhibited a line-broadening in many peaks from the C-terminal segment, which is a characteristic of molten globule states, suggesting the unstable nature of its C-terminal α-helical structure. As the concentration of the CAHS1 protein increased, these broader peaks disappeared, rendering only the narrower peaks that originated from the N-terminal disordered segments observable (Fig. 2A). These data indicate that the CAHS1 protein forms condensates through its C-terminal helical region, leaving the remaining regions mobile and disordered.

To observe this sol–gel transition phenomena in a mesoscopic view, we performed a real-time observation of the CAHS1 protein oligomerization using high-speed atomic force microscopy (HS-AFM). Under dilute conditions, the CAHS1 protein was monomeric, consisting of a flexible disordered part and a globular region (Supporting Movie S1). In contrast, the CAHS1 protein formed fibrils when its concentration was increased (from 0.4 μM to 3.3 μM) (Fig. 2B, Supporting Movie S2). Such fibril formation was observed for CAHS1-C but not CAHS1-N (Supporting Fig. S1D). Furthermore, the HS-AFM data indicate that the CAHS1 fibrils disappeared upon the addition of 50 mM KCl, indicating the reversible nature of fibril formation (Supporting Movie S3). These data indicate that the CAHS1 proteins assembled into fibrous structures through their C-terminal helical regions, leading to gel formation.

Fibril formation of the CAHS1 protein in vivo. The in vitro experimental data showed that CAHS1 proteins assembled into fibrils at high concentrations in solution as well as under desiccating conditions. We further examined the potential ability of the CAHS1 protein to form aggregates under molecular crowding condition in cells. In a previous report, the bacterial expression of CAHS proteins from *H. exemplaris* resulted in an improved tolerance of bacterial cells to desiccation[34]. Hence, we overexpressed the CAHS1 protein from *R. varieornatus* with an N-terminal FLAG tag (FLAG-CAHS1) in *Escherichia coli* BL21(DE3) as a model system and subjected it to TEM observation. The TEM images visualized the intracellular fibril structures with approximately 10-nm width (Supporting Fig. S2), confirming that CAHS1 proteins can form fibrils in cells.

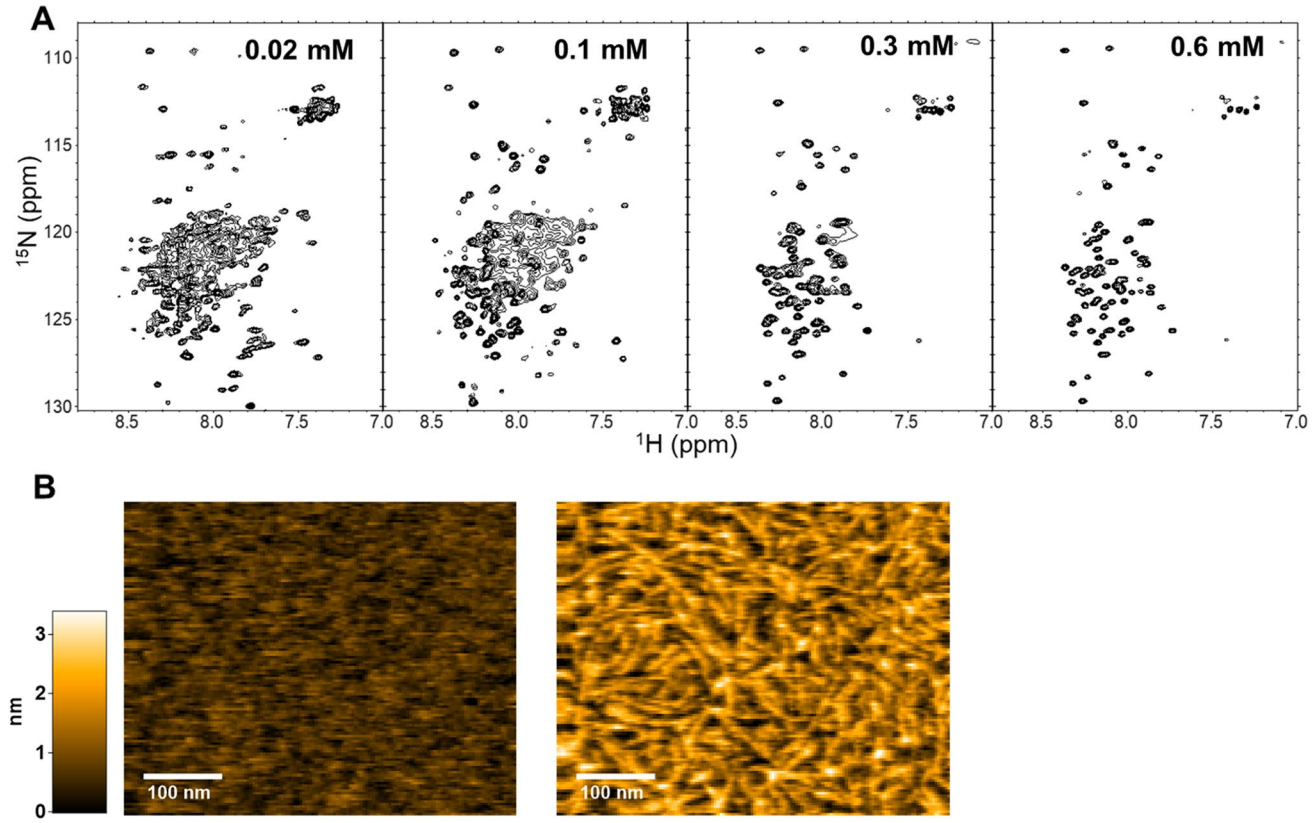

Figure 2. Fibril formation of the CAHS1 protein in vitro. (**A**) ^{1}H-^{15}N HSQC spectra of the CAHS1 protein at protein concentrations of 0.02, 0.1, 0.3, and 0.6 mM. (**B**) Typical HS-AFM images of CAHS1 protein fibrils. Left: the HS-AFM image of the mica surface with CAHS1 protein at a final concentration of 0.4 μM, about 3 min after injection into the observation solution. Right: the HS-AFM image about 2 min after the addition of CAHS1 protein at a final concentration of 3.3 μM.

We hypothesized that the fibril formation of CAHS1 protein in cells is associated with an improved tolerance against various water stresses, such as dehydration and hyperosmotic treatment. Therefore, we attempted to assess the relationship between the condensation of CAHS1 protein and hyperosmotic stress. For this purpose, the CAHS1 protein with a C-terminal FLAG (CAHS1-FLAG) was overexpressed in HeLa cells, which were used because of their stress-sensitive and easily observable properties. Immunostaining with anti-FLAG antibody visualized the cytoplasmic distribution of the recombinant CAHS1 protein (Supporting Fig. S3), which is consistent with a previous study[32]. After the hyperosmotic shock with 0.5 M sorbitol, the CAHS1-FLAG proteins were deposited as approximately 650-nm particles.

Furthermore, for live imaging, the CAHS1 protein fused to a C-terminal mEGFP protein (CAHS1-mEGFP) was overexpressed in HeLa cells. The fluorescence-labeled CAHS1 proteins were distributed evenly throughout the cytoplasm in the absence of osmotic stresses, but these were rapidly assembled into bright particles in both cytoplasm and nucleus by a 0.5 M sorbitol-induced osmotic shock (Fig. 3, Supporting Movie S4). Upon the removal of sorbitol by buffer replacement, the particles disappeared, indicating that the protein condensation was reversible. We confirmed that the reversible condensate formation was induced also by addition of 0.2 M sodium chloride as another osmolyte and depended on the existence of CAHS1 (Fig. 3 and Supporting Movies S4 and S5). As a control, HeLa cells expressing mEGFP or HaloTag-fused mEGFP was treated with the osmolytes, showing that the hyperosmotic stimulation did not alter the cytoplasmic localization of these fluorescent proteins while inducing aggregate formation in the nucleus. These data indicate that the CAHS1 proteins reversibly form particles in cytosols under desiccation-mimicking conditions.

Discussion

In this study, the self-assembling property of CAHS1 protein was characterized in vitro and in vivo. The in vitro data indicated that the CAHS1 proteins homo-oligomerized via their C-terminal α-helical regions as their concentration increases. The HS-AFM data clearly visualized the fibril formation process of this protein. Furthermore, the in vivo observation demonstrated that the overexpressed CAHS1-mEGFP proteins formed condensates in an osmotic shock-dependent manner. At higher protein concentrations, the CAHS1 proteins formed a hydrogel presumably associated with its condensation. These data suggest that, upon drying, the CAHS1 proteins form oligomers and eventually undergoes sol–gel transition in cytosolic environments. The present data also showed that the α-helical fibrous network of the CAHS1 protein can be formed in *E. coli* cells and are

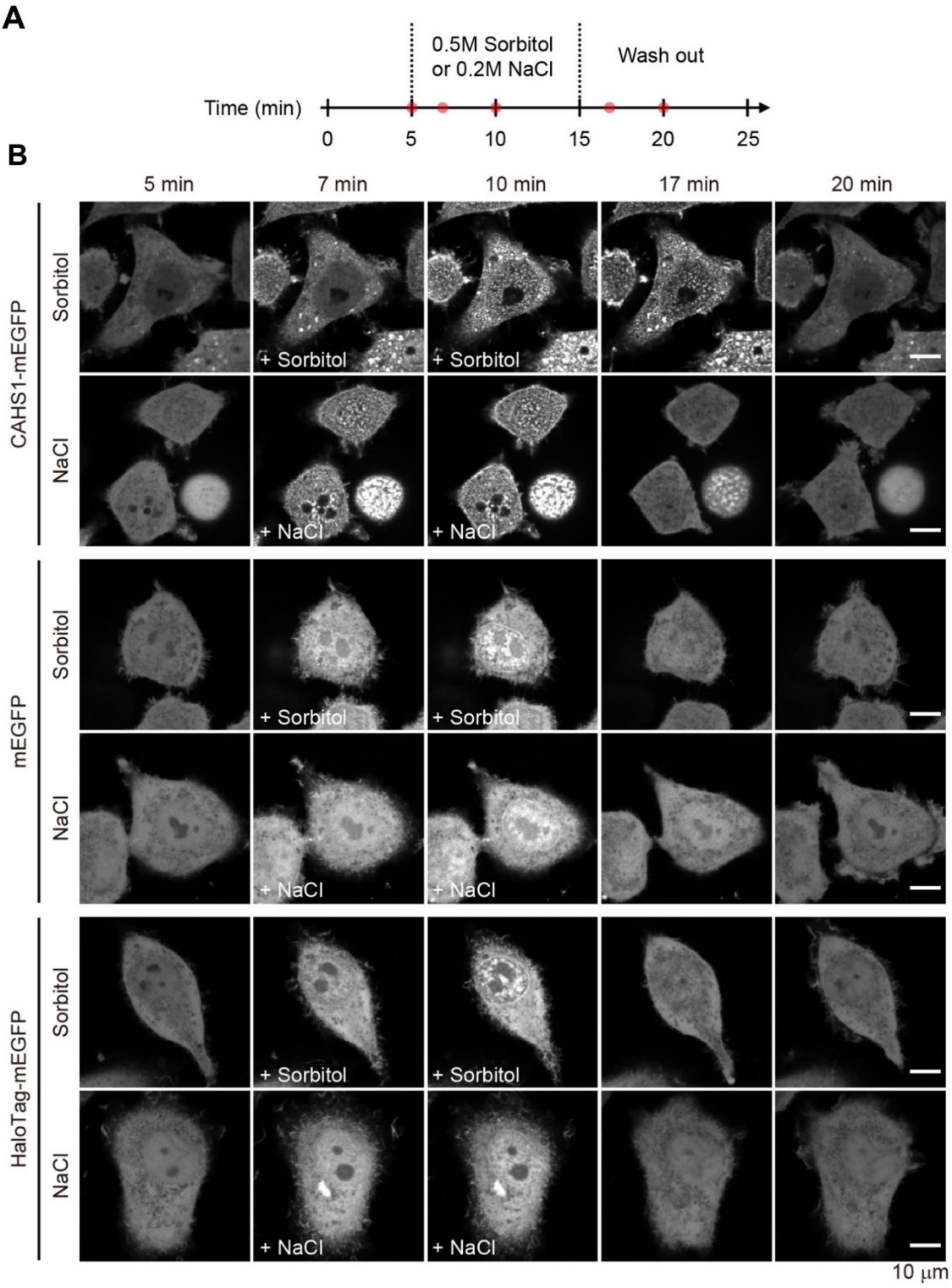

Figure 3. Real-time monitoring of the reversible formation of CAHS1 protein particles. (**A**) Timeline of time-laps imaging with hyperosmotic shock. The red dots represent the time points when the representative cells are presented in panel (**B**). (**B**) Time-laps images of HeLa cells overexpressing the CAHS1-mEGFP, mEGFP, and Halo Tag-mEGFP proteins. A sorbitol or sodium chloride solution was added at 5 min. After 10 min, the cells were washed with a flesh medium using a microfluidics system.

maintained even in desiccated conditions. These molecular assembling processes are reversible, depending on solution pH, temperature, and salt concentration.

The multistep phase transition of the CAHS1 protein suggests its multifunctional property. In particular, the CAHS1 fibril formation implies that the anhydrobiotic functions of this protein are distinct from those of trehalose, i.e., water replacement and/or vitrification. Indeed, although the CAHS protein vitrification was hypothesized to be a key mechanism[34], the interpretation of the data leading to such hypothesis has been negated[37]. The osmotic shock-induced formation of cytosolic coacervate-like droplets is reminiscent of the stress granules, which are supposed to protect the mRNAs under stress conditions[38]. It has recently been reported that a LEA protein from *A. franciscana* forms droplets incorporating positively charged fluorescent protein[39]. The present study along with this report suggests that the liquid–liquid phase separation involving the protein assembly promotes the desiccation tolerance through reversible formation of protective compartments for desiccation-sensitive biomolecules. In these compartments, the CAHS1 proteins presumably form a fibrous network with a water-holding capacity that is resistant to desiccation. Moreover, under extremely anhydrobiotic conditions, the CAHS1 network may act as a "dry chaperone", which not only protects the desiccation-sensitive proteins against denaturation, but also maintains the integrity of other biomolecular complexes, including RNAs and membranes.

We thus propose that, like the LEA proteins, the CAHS1 proteins form cytosolic fibrous condensates, which presumably have variable mechanisms for the desiccation tolerance. There exist a series of LEA-like proteins, including the CAHS-family proteins, which exhibit different cellular distributions and subcellular localizations[23,32,33]. These proteins may have different assembling properties from those of the CAHS1 proteins, playing distinct roles in a coordinated manner in anhydrobiotic processes. Furthermore, our recent multi-omics study of the heterotardigrade *Echiniscus testudo* identified two families of novel abundant heat-soluble proteins. Despite no sequence homology, these proteins share analogous structural characteristics with the eutardigrade CAHS proteins[36]. A comprehensive characterization of these proteins is currently underway in our groups. The present study thus provides new insights into molecular strategies of organisms to adapt to extreme environments.

Materials and methods

Expression and purification of CAHS1 protein. The plasmid vector encoding the *R. varieornatus* CAHS1 protein was constructed and cloned as a fusion protein with a hexahistidine (His_6) tag at the N-terminus using a pET28a vector (Novagen, Merck). CAHS1-N (Met1-Ser96) and CAHS1-C (Pro97-His237) were constructed using standard genetic engineering techniques with a His_6 tag at the N-terminus using the pET28a vector (Novagen, Merck). The recombinant CAHS1 protein, CAHS1-N, and CAHS1-C were expressed in the *E. coli* BL21(DE3) strain in Luria Bertani media. For the production of ^{15}N-labeled proteins, cells were grown in M9 minimal media containing $[^{15}N]NH_4Cl$ (1 g/L). After sonication, the supernatant was incubated at 90 °C for 30 min; then, heat-soluble and -insoluble fractions were separated by centrifugation. The His_6-tag fusion proteins were purified with a cOmplete™ His-tag purification resin (Roche, Merck). The fusion proteins were cleaved by incubation with thrombin protease (Sigma-Aldrich) and purified with a Superdex 200 pg (Cytiva) with 10 mM potassium phosphate buffer (pH 7.0).

NMR measurements. The NMR spectral measurements were made on a Bruker DMX-500 spectrometer equipped with a cryogenic probe. The probe temperature was set to 5 °C. ^{15}N-labeled CAHS1 protein, CAHS1-N, and CAHS1-C were dissolved at a protein concentration of 0.1 mM in 20 mM potassium phosphate buffer (pH 7.0) containing 5% (v/v) ^2H_2O.

CD measurements. The CD spectra were measured at 25 °C on a JASCO J-720WI apparatus using a 1.0-mm path length quartz cell. The CAHS1 protein, CAHS1-N, and CAHS1-C were dissolved at a protein concentration of 10 μM in 20 mM potassium phosphate buffer (pH 7.0).

Turbidity measurements. The CAHS1 protein in various conditions were added to a 96-well microplate (Corning, #4442). The optical density of the CAHS1 protein was measured at 25 °C at 595 nm by a multi-mode microplate reader (Infinite 200 PRO, TECAN). The CAHS1 protein was dissolved at protein concentrations of 0.02, 0.1, 0.3, 0.6, and 1.1 mM in 20 mM potassium phosphate buffer (pH 8.0, 7.0, 6.0, or 5.0) with or without 150 mM NaCl.

IR measurements. Attenuated total reflection-Fourier transform infrared measurements were performed using an FTIR spectrometer (VERTEX70, Bruker Optics) equipped with a mercury-cadmium-telluride detector. A 5 μL aliquot of 40 μM CAHS1 proteins (1.1 mg/mL) in ultrapure water was placed on the surface of a diamond ATR crystal with three internal reflection (DurasamplIR II, Smiths Detection) and dried under a gentle stream of N_2 gas. After the spectral measurements of dried state of CAHS1 proteins, two 2 μL aliquots of D_2O or glycerol-OD_3/D_2O mixture solution were placed beside the ATR crystal surface and sealed together with the CAHS1 sample by a CaF_2 window (25-mm diameter and 2-mm thickness) and silicone spacer to control the hydration level of the CAHS1 samples through saturated heavy water vapor. Varying amounts of glycerol-OD_3 liquid (Sigma, purity 99.0%) were mixed with D_2O to obtain glycerol/water solutions with 0–50 volume % of glycerol, which enabled the regulation of the saturated vapor pressure in a closed compartment[40]. Using D_2O instead of H_2O, the amide I band of proteins was observed free from interference with the OH bending mode of water. After 5 min, the spectra were measured at 25 °C. Each spectrum was collected with a spectral resolution of 2 cm^{-1} in the 4000–700 cm^{-1} region by averaging 32 scans of interferograms. A background spectrum was

recorded with an empty ATR crystal before the measurement of samples. The second derivatives of the spectral data were analyzed by an IGOR Pro software.

HS-AFM. The HS-AFM images of the CAHS1 proteins were acquired in a tapping mode using a laboratory-built HS-AFM apparatus and a short cantilever (Olympus: BL-AC10;9-μm long, 2-μm wide, and 130-nm thick, 500 kHz-600 kHz resonance frequency in observation buffer, 0.1 N/m spring constant) at 25 °C. To observe its monomeric structure, the CAHS1 protein was dissolved at a concentration of 10 nM in 10 mM potassium phosphate buffer (pH 7.4) and deposited on a freshly cleaved mica surface. To observe the fibril formation of the CAHS1 protein at its higher concentrations, the mica substrates with 0.4-μM CAHS1 protein in pure water was imaged, and after about 3 min, the CAHS1 protein solution was added to the solution so that the final concentration was 3.3 μM. The HS-AFM observation of CAHS1-N was performed in the same way as for the full-length CAHS1 protein. For HS-AFM observation of CAHS1-C, the mica substrates with 2-μM CAHS1-C were imaged in 10 mM sodium phosphate buffer (pH 7.4). To investigate the reversibility of fibril formation, 50 mM KCl was added to the CAHS1 fibrils.

TEM. FLAG-CAHS1 was constructed using standard genetic engineering techniques with an N-terminal FLAG using a pT7-FLAG-1 vector (Sigma-Aldrich, Merck). The bacterial cells of *E. coli* BL21(DE3) strain transformed with FLAG-CAHS1 plasmids were cultured in M9 minimal media at 37 °C under constant shaking. Protein expression was induced by adding 0.5 mM isopropyl-β-D-thiogalactopyranoside when the absorbance reached 0.8 at 600 nm. After 4 h, the cells were harvested and washed twice with 50 mM Tris–HCl (pH 8.0) and 150 mM NaCl. The control was run without the FLAG-CAHS1 plasmid.

Cell pellets collected were fixed with 2.5% glutaraldehyde in 10 mM Tris–HCl (pH 8.0) for 30 min at 23 °C and collected by centrifugation at 5,000 g for 5 min. The cells were washed with distilled water three times to remove glutaraldehyde and fixed with 2% osmium tetroxide at 23 °C for 1 h. After washing with distilled water, fixed cells were stained with 1% uranyl acetate for 20 min. Then, after washing with distilled water, cells were collected by centrifugation at 5,000 g for 3 min. Next, the pellet was embedded in 2% low melting point agar medium (Sigma Aldrich, St. Louis, Missouri, USA), then the cell-containing agar medium was cut into small pieces of approximately 1–2 mm and dehydrated with a stepwise ethanol series (50%, 60%, 70%, 80%, 90%, 95%, and 100%). The sample was infiltrated with QY-1 (Nissin EM Co. Ltd.), embedded in epoxy resin (Durcupan: Sigma-Aldrich), and polymerized at 60 °C for 2 days. Ultrathin sections (approximately 70 nm thick) were prepared with a diamond knife and collected on a Formvar-coated Cu single slot grid. Sections were stained with 2% uranyl acetate and 0.5% lead citrate and observed with a transmission electron microscope (JEM1010, JEOL) at an accelerated voltage of 80 kV.

Immunofluorescence measurements. The plasmid DNA expressing the CAHS1-FLAG (pCAGGS-CAHS1-FLAG) protein was transfected into HeLa Italy cells with 293fectin transfection reagent (Thermo Fisher Scientific). The cells were seeded on 4-well glass-base dishes (Greiner) and cultured in Dulbecco's modified Eagle's medium (DMEM) supplemented with 10% fetal bovine serum (FBS). After one day, the cells were treated with or without 0.5 M sorbitol in DMEM supplemented with 10% FBS for 5 min. The cells were fixed with 4% paraformaldehyde in phosphate-buffered saline (PBS) for 15 min and were permeabilized with 0.5% Triton X-100 in PBS for 15 min at 25 °C. After blocking with 5% goat serum (Abcam, ab7481) in PBS for 1 h at 25 °C, the cells were incubated with monoclonal mouse ANTI-FLAG® M2 antibody (Sigma-Aldrich, F1804-50UG, dilution 1:100) overnight at 4 °C and then with Alexa Fluor 488-conjugated goat anti-mouse IgG antibody (Thermo Fisher Scientific, A32723, dilution 1:1000) for 1 h in PBS containing 5% goat serum 25 °C.

Time-laps imaging with hyperosmotic shock. HeLa cells were seeded on collagen-coated 35-mm glass-base dishes (IWAKI). The plasmid expressing the CAHS1-mEGFP protein (pCAGGS-CAHS1-mEGFP), mEGFP (pCAGGS-CAHS1-mEGFP), or Halo Tag-mEGFP (pCAGGS-Halo-GGSGG-mEGFP) was transfected into the HeLa cells with 293fectin transfection reagent (Invitrogen). After 48 h, the medium was replaced with an imaging medium (FluoroBrite DMEM, Thermo Fisher Scientific) supplemented with 1% GlutaMAX (Thermo Fisher Scientific) and 0.1% bovine serum albumin.

For hyperosmotic shock experiments using microfluidic plates (Merck, CellASIC® ONIX M04S-03), the cells were initially observed in an imaging medium. Then, 0.5 M sorbitol or 0.2 M sodium chloride was added 5 min after starting the observations. After 10 min of incubation in 0.5 M sorbitol, the medium was replaced with an imaging medium, and the cells were observed for another 10 min. The images were acquired every 10 s.

Fluorescence imaging. The cells were imaged with an IX83 inverted microscope (Olympus, Tokyo) equipped with an sCMOS camera (Prime, Photometrics, Tucson, AZ), a spinning disk confocal unit (CSU-W1; Yokogawa Electric Corporation, Tokyo), and diode lasers at a wavelength of 488 nm. An oil immersion objective lens (UPLXAPO60XO, N.A. 1.42; Olympus) was used. The excitation laser and fluorescence filter settings were as follows: excitation laser, 488 nm; dichroic mirror (DM), 405/488/561 nm; and emission filters, 500–550 nm. During the observation, live cells were incubated with a stage incubator containing 5% CO_2 (STXG-IX3WX; Tokai Hit) at 37 °C.

Received: 16 July 2021; Accepted: 11 October 2021
Published online: 04 November 2021

References

1. Hibshman, J. D., Clegg, J. S. & Goldstein, B. Mechanisms of desiccation tolerance: Themes and variations in brine shrimp, roundworms, and tardigrades. *Front. Physiol.* **11**, 592016. https://doi.org/10.3389/fphys.2020.592016 (2020).
2. Rapoport, A., Golovina, E. A., Gervais, P., Dupont, S. & Beney, L. Anhydrobiosis: Inside yeast cells. *Biotechnol. Adv.* **37**, 51–67. https://doi.org/10.1016/j.biotechadv.2018.11.003 (2019).
3. Janis, B., Belott, C. & Menze, M. A. Role of intrinsic disorder in animal desiccation tolerance. *Proteomics* **18**, e1800067. https://doi.org/10.1002/pmic.201800067 (2018).
4. Garcia, A. H. Anhydrobiosis in bacteria: From physiology to applications. *J. Biosci.* **36**, 939–950. https://doi.org/10.1007/s12038-011-9107-0 (2011).
5. Guidetti, R. & Jönsson, K. I. Long-term anhydrobiotic survival in semi-terrestrial micrometazoans. *J. Zool. Lond.* **257**, 181–187 (2002).
6. Keilin, D. The problem of anabiosis or latent life: History and current concept. *Proc. R. Soc. Lond. B Biol. Sci.* **150**, 149–191. https://doi.org/10.1098/rspb.1959.0013 (1959).
7. Alpert, P. Constraints of tolerance: Why are desiccation-tolerant organisms so small or rare?. *J. Exp. Biol.* **209**, 1575–1584. https://doi.org/10.1242/jeb.02179 (2006).
8. Schill, R. O. *et al.* Molecular mechanisms of tolerance in tardigrades: New perspectives for preservation and stabilization of biological material. *Biotechnol. Adv.* **27**, 348–352. https://doi.org/10.1016/j.biotechadv.2009.01.011 (2009).
9. Hand, S. C., Menze, M. A., Toner, M., Boswell, L. & Moore, D. LEA proteins during water stress: Not just for plants anymore. *Annu. Rev. Physiol.* **73**, 115–134. https://doi.org/10.1146/annurev-physiol-012110-142203 (2011).
10. Clegg, J. S. The origin of trehalose and its significance during the formation of encysted dormant embryos of *Artemia salina*. *Comp. Biochem. Physiol.* **14**, 135–143. https://doi.org/10.1016/0010-406x(65)90014-9 (1965).
11. Lapinski, J. & Tunnacliffe, A. Anhydrobiosis without trehalose in bdelloid rotifers. *FEBS Lett.* **553**, 387–390. https://doi.org/10.1016/s0014-5793(03)01062-7 (2003).
12. Sakurai, M. *et al.* Vitrification is essential for anhydrobiosis in an African chironomid, Polypedilum vanderplanki. *Proc. Natl. Acad. Sci. U. S. A.* **105**, 5093–5098. https://doi.org/10.1073/pnas.0706197105 (2008).
13. Honda, Y., Tanaka, M. & Honda, S. Trehalose extends longevity in the nematode *Caenorhabditis elegans*. *Aging Cell* **9**, 558–569. https://doi.org/10.1111/j.1474-9726.2010.00582.x (2010).
14. Moore, D. S., Hansen, R. & Hand, S. C. Liposomes with diverse compositions are protected during desiccation by LEA proteins from *Artemia franciscana* and trehalose. *Biochim. Biophys. Acta* **104–115**, 2016. https://doi.org/10.1016/j.bbamem.2015.10.019 (1858).
15. Crowe, J. H., Carpenter, J. F. & Crowe, L. M. The role of vitrification in anhydrobiosis. *Annu. Rev. Physiol.* **60**, 73–103. https://doi.org/10.1146/annurev.physiol.60.1.73 (1998).
16. Goyal, K. *et al.* Transition from natively unfolded to folded state induced by desiccation in an anhydrobiotic nematode protein. *J. Biol. Chem.* **278**, 12977–12984. https://doi.org/10.1074/jbc.M212007200 (2003).
17. Caramelo, J. J. & Iusem, N. D. When cells lose water: Lessons from biophysics and molecular biology. *Prog. Biophys. Mol. Biol.* **99**, 1–6. https://doi.org/10.1016/j.pbiomolbio.2008.10.001 (2009).
18. Goyal, K., Walton, L. J. & Tunnacliffe, A. LEA proteins prevent protein aggregation due to water stress. *Biochem. J.* **388**, 151–157. https://doi.org/10.1042/BJ20041931 (2005).
19. Chakrabortee, S. *et al.* Intrinsically disordered proteins as molecular shields. *Mol. Biosyst.* **8**, 210–219. https://doi.org/10.1039/c1mb05263b (2012).
20. Erkut, C. *et al.* Molecular strategies of the *Caenorhabditis elegans* Dauer Larva to survive extreme desiccation. *PLoS ONE* **8**, e82473. https://doi.org/10.1371/journal.pone.0082473 (2013).
21. Møbjerg, N. *et al.* Survival in extreme environments - on the current knowledge of adaptations in tardigrades. *Acta Physiol. (Oxf.)* **202**, 409–420. https://doi.org/10.1111/j.1748-1716.2011.02252.x (2011).
22. Møbjerg, N. & Neves, R. C. New insights into survival strategies of tardigrades. *Comp. Biochem. Physiol. A Mol. Integr. Physiol.* **254**, 110890. https://doi.org/10.1016/j.cbpa.2020.110890 (2021).
23. Hesgrove, C. & Boothby, T. C. The biology of tardigrade disordered proteins in extreme stress tolerance. *Cell Commun. Signal* **18**, 178. https://doi.org/10.1186/s12964-020-00670-2 (2020).
24. Schokraie, E. *et al.* Investigating heat shock proteins of tardigrades in active versus anhydrobiotic state using shotgun proteomics. *J. Zool. Syst. Evol. Res.* **49**, 111–119 (2011).
25. Kamilari, M., Jørgensen, A., Schiøtt, M. & Møbjerg, N. Comparative transcriptomics suggest unique molecular adaptations within tardigrade lineages. *BMC Genom.* **20**, 607. https://doi.org/10.1186/s12864-019-5912-x (2019).
26. Yoshida, Y. *et al.* A novel Mn-dependent peroxidase contributes to tardigrade anhydrobiosis. *bioRxiv* https://doi.org/10.1101/2020.1111.1106.370643 (2020).
27. Rizzo, A. M. *et al.* Antioxidant defences in hydrated and desiccated states of the tardigrade *Paramacrobiotus richtersi*. *Comp. Biochem. Physiol. B Biochem. Mol. Biol.* **156**, 115–121. https://doi.org/10.1016/j.cbpb.2010.02.009 (2010).
28. Halberg, K. A., Jørgensen, A. & Møbjerg, N. Desiccation tolerance in the tardigrade *Richtersius coronifer* relies on muscle mediated structural reorganization. *PLoS ONE* **8**, e85091. https://doi.org/10.1371/journal.pone.0085091 (2013).
29. Hengherr, S., Heyer, A. G., Kohler, H. R. & Schill, R. O. Trehalose and anhydrobiosis in tardigrades–evidence for divergence in responses to dehydration. *FEBS J.* **275**, 281–288. https://doi.org/10.1111/j.1742-4658.2007.06198.x (2008).
30. Yoshida, Y. *et al.* Comparative genomics of the tardigrades *Hypsibius dujardini* and *Ramazzottius varieornatus*. *PLoS Biol.* **15**, e2002266. https://doi.org/10.1371/journal.pbio.2002266 (2017).
31. Förster, F. *et al.* Tardigrade workbench: Comparing stress-related proteins, sequence-similar and functional protein clusters as well as RNA elements in tardigrades. *BMC Genom.* **10**, 469. https://doi.org/10.1186/1471-2164-10-469 (2009).
32. Yamaguchi, A. *et al.* Two novel heat-soluble protein families abundantly expressed in an anhydrobiotic tardigrade. *PLoS ONE* **7**, e44209. https://doi.org/10.1371/journal.pone.0044209 (2012).
33. Tanaka, S. *et al.* Novel mitochondria-targeted heat-soluble proteins identified in the anhydrobiotic Tardigrade improve osmotic tolerance of human cells. *PLoS ONE* **10**, e0118272. https://doi.org/10.1371/journal.pone.0118272 (2015).
34. Boothby, T. C. *et al.* Tardigrades use intrinsically disordered proteins to survive desiccation. *Mol. Cell* **65**, 975–984. https://doi.org/10.1016/j.molcel.2017.02.018 (2017).
35. Kondo, K., Kubo, T. & Kunieda, T. Suggested involvement of PP1/PP2A activity and de novo gene expression in anhydrobiotic survival in a tardigrade, *Hypsibius dujardini*, by chemical genetic approach. *PLoS ONE* **10**, e0144803. https://doi.org/10.1371/journal.pone.0144803 (2015).
36. Murai, Y. *et al.* Multiomics study of a heterotardigrade, *Echinisicus testudo*, suggests convergent evolution of anhydrobiosis-related proteins in Tardigrada. *bioRxiv* https://doi.org/10.1101/2020.10.27.358333 (2020).
37. Arakawa, K. & Numata, K. Reconsidering the "glass transition" hypothesis of intrinsically unstructured CAHS proteins in desiccation tolerance of tardigrades. *Mol. Cell* **81**, 409–410. https://doi.org/10.1016/j.molcel.2020.12.007 (2021).

38. Hofmann, S., Kedersha, N., Anderson, P. & Ivanov, P. Molecular mechanisms of stress granule assembly and disassembly. *Biochim. Biophys. Acta Mol. Cell Res.* **1868**, 118876. https://doi.org/10.1016/j.bbamcr.2020.118876 (2021).
39. Belott, C., Janis, B. & Menze, M. A. Liquid-liquid phase separation promotes animal desiccation tolerance. *Proc. Natl. Acad. Sci. U. S. A.* **117**, 27676–27684. https://doi.org/10.1073/pnas.2014463117 (2020).
40. Noguchi, T. & Sugiura, M. Flash-induced FTIR difference spectra of the water oxidizing complex in moderately hydrated photosystem II core films: effect of hydration extent on S-state transitions. *Biochemistry* **41**, 2322–2330. https://doi.org/10.1021/bi011954k (2002).

Acknowledgements

We are grateful for Takahiro Bino (NIBB) for help in immunofluorescence measurements and fluorescence imaging. We would like to thank Sachiko Yamada (NIPS) for help in preparation of specimens for TEM experiments. We also thank Yuikiko Isono (IMS) for help in preparation of recombinant proteins. *Chlorella vulgaris* used to feed the tardigrades were partly provided by courtesy of Chlorella Industry Inc. This work was supported in part by JSPS KAKENHI (Grant Number JP19K07041 to M.Y-U, and JP17H03620 and JP21H05279 to K.Arakawa), JST CREST (Grant Number JPMJCR17N5 to Y.F.), funds from the Nanotechnology Platform Program (Molecule and Material Synthesis) of the Ministry of Education, Culture, Sports, Science, and Technology (MEXT), Japan, funds from Yamagata Prefectural Government and Tsuruoka City, funds from IMS-IIPA internship program to E.W.G., and funds from ENSCP internship program to V.S. This work was also supported by the Joint Research of the Exploratory Research Center on Life and Living Systems (ExCELLS) (ExCELLS program No. 18-207, 19-208, and 19-501 to K.Arakawa, No. 18-101 to T.U.), by Instrument Center of IMS, by the EM facility in NIPS, and by the Functional Genomics Facility of the NIBB Core Research Facilities.

Author contributions

M.Y.-U., K.Aoki, K.Arakawa, K. K. designed of research; M.Y.-U., K.Aoki, K.Arakawa, K.K. wrote the paper; M.Y.-U., S.N., V.S., E.G., S.Y., and T.S. performed protein expression and purification; M.Y.-U., S.N., V.S., E.G., and T.S. performed NMR, CD, and turbidity measurements; H.W., C.G., and T.U. performed HS-AFM; M.Y.-U., S.Y., and Y.F. performed IR; C.S. and K.M. performed EM; S.T. and K.Aoki performed fluorescence measurements.

Competing interests

The authors declare no competing interests.

Additional information

Supplementary Information The online version contains supplementary material available at https://doi.org/10.1038/s41598-021-00724-6.

Correspondence and requests for materials should be addressed to K.K.

Reprints and permissions information is available at www.nature.com/reprints.

Publisher's note Springer Nature remains neutral with regard to jurisdictional claims in published maps and institutional affiliations.